A STUDY OF e^+e^- ANNIHILATION INTO HADRONS IN THE 1550-2200 MeV ENERGY RANGE WITH THE MAGNETIC DETECTOR DM1 AT DCI†

B. Delcourt, J.L. Bertrand, D. Bisello*, J.C. Bizot, J. Buon,
A. Cordier, I. Derado**, P. Eschstruth, L. Fayard, J. Jeanjean,
M. Jeanjean, F. Mané, J.C. Parvan, M. Ribes, F. Rumpf
Laboratoire de l'Accélérateur Linéaire
91405 - Orsay, FRANCE

ABSTRACT

We present here the results obtained with the Magnetic Detector DM1 on the Orsay e^+e^- colliding beams (DCI) for $1550 < \sqrt{S} < 2180$ MeV. The total integrated luminosity is 1100 nb^{-1} over the whole energy range. Kinematics of annihilation events are determined from momentum measurements on the charged particles with an accuracy $\Delta p/p \simeq 2.5\%$ at 500 MeV/c over a solid angle $\Omega = .6 \times 4\pi$ sr.

Cross sections are given for e^+e^- annihilation into $p\bar{p}$, into four and five pions ($\pi^+\pi^-\pi^+\pi^-$ including $\rho^o\pi^+\pi^-$, $\pi^+\pi^-\pi^+\pi^-\pi^o$ including $\omega\pi^+\pi^-$), and into storage mesons K^+K^-, $K^o_S K^o_L$, KK^*, $K\bar{K}\pi\pi$ including $K^*K\pi$, inclusive K^o_S). Limits on rare channels like baryonium states $\phi^o\pi^o$, $\phi^o\eta^o$ are also obtained.

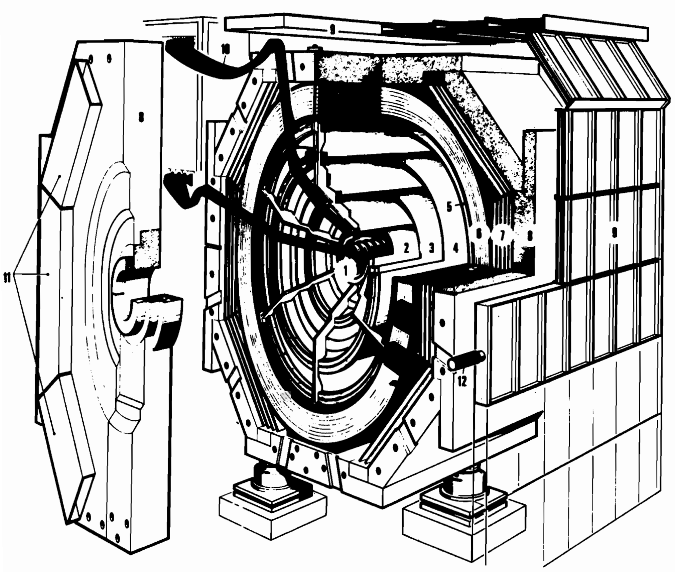

FIG.1 - Cut away view of the DMA Detector.

1) Vacuum chamber.
2)3)4)5) Cylindrical Multiwire proportional chambers
6) Magnet Solenoïd. 7) Drift chambers.
8) Magnet Yoke. 9) Cosmic ray veto system.
10) Striplines connecting the wires to the amplifiers.

The set up

Data taking with the Magnetic Detector DM1 on the DCI colliding beam rings began in April 1978.

The detector[1], shown in Fig. 1, consists of four concentric cylindrical multiwire proportional chambers in a uniform magnetic field of .82T and covers a solid angle of $.6 \times 4\pi$ sr. In each chamber both the azimuthal angle (in a plane normal to the beam line) and the longitudinal coordinate (along the beam line) of charged particle impacts are measured, with accuracy $r\Delta\phi = .7$mm and $\Delta z = 2$ mm respectively. The thickness of each chamber is $.7 \times 10^{-3}$ Radiation Length, the vacuum chamber thickness being 12×10^{-3} R.L. The trigger requires that at least two charged particles reach the third chamber (75 MeV/c for the minimum transverse momentum). The system detects charged particles and measures their momentum with an accuracy $\frac{\Delta p}{p} = \frac{p}{500 \text{ MeV/c}} \times 2.5\%$. Twenty five scintillators surrounding the magnet are used to eliminate cosmic ray background by time of flight.

For every event we measure the time difference between the beam collision and the chamber signal. This allows us to make a very accurate estimate of the contamination of two body channels (e^+e^-, $p\bar{p}$, K^+K^-) by unidentified cosmic rays : the jitter of the chambers is 30 ns and the time between collisions is 316 ns.

We used only the lower of the two DCI rings. The luminosity has been improved during the past year and now reaches 4.8×10^{29} cm^{-2} s^{-1} at 1.8 GeV total energy. Data were taken in energy steps of the same order as the beam dispersion (1 to 2 MeV total energy). The results were combined in wider intervals to get enough statistics. The energy intervals chosen are indicated by horizontal bars in the figures. The total analysed luminosity is 1100 nb^{-1} over the energy regions 1550-2060 and 2110-2180 MeV.

Selection of channels

Charged two body events (e^+e^-, K^+K^-, $p\bar{p}$) are selected by cuts on the angle ζ between the two tracks, the difference Δp between the two momenta, and the average value p_A of the two momenta. Typical cuts are $|\zeta - 180°| < 5°$ to $10°$, $\Delta P/p_A < 7$ to 15 %, and p_A equal to the predicted value within 7 to 10 %.

Charged four body events ($\pi^+\pi^-\pi^+\pi^-$, $K^o_S(\to\pi^+\pi^-)$, $K^\pm\pi^\mp$, $K^+K^-\pi^+\pi^-$) are selected in three or four visible tracks. In the case of four visible tracks, cuts are applied on total momentum and reconstructed energy (calculated under an assumption about the identity of the particles) (Fig.2). For three visible tracks (not yet used for $K^+K^-\pi^+\pi^-$) cuts are applied on reconstructed energy with the momentum of the unseen particle set equal to the missing momentum (Fig. 3).

† Work supported by the "Institut National de Physique Nucléaire et de Physique des Particules".
* On leave from Istituto di Fisica, ISN Sezione di Padova, Italy.
** Present address : Max Planck Institut für Physik, D8 München 40, Germany.

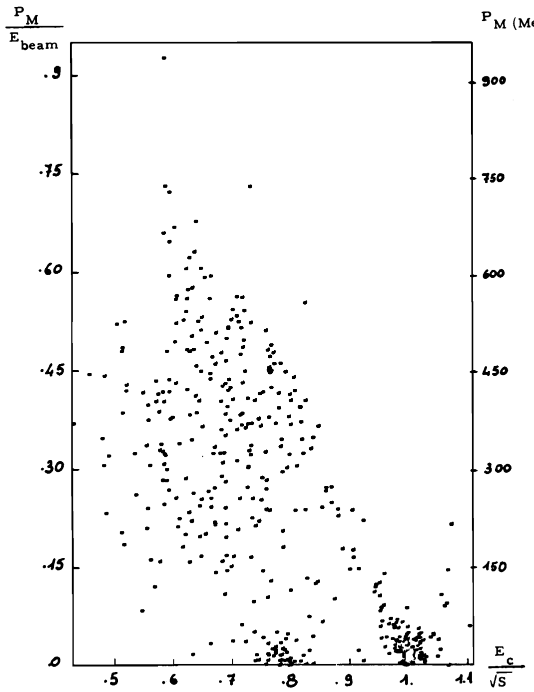

FIG.2 - Scatter plot of four prong events for 2002 MeV < $\sqrt{S}$ < 2060 MeV. Total momentum P_M vs computed energy E_L of the 4 particles assumed to be pions.

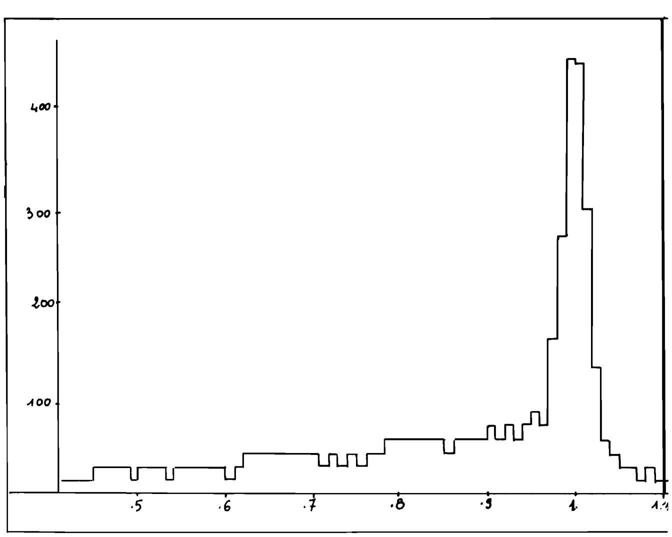

FIG.3 - Three track pion events - computed energy divided by energy of the two beams, assuming the missing particle to be a pion - 1600 < $\sqrt{S}$ < 1700 MeV.

For $\pi^+\pi^-\pi^+\pi^-\pi^\circ$, special care must be taken to avoid contamination by radiative four charged pion events. Thus we require a minimum missing momentum (12% of the energy of one beam) and a minimum angle between the missing momentum and the beam line (10°).

K^o_S are identified by their decay into $\pi^+\pi^-$. In order to suppress background from pion events, a minimum distance of 6 mm from the decay vertex to the beam line is required. Cuts are also applied to the angle between the two pions and to the direction of their total momentum. The background below the K^o_S mass is estimated from side bins and subtracted (Fig.4).

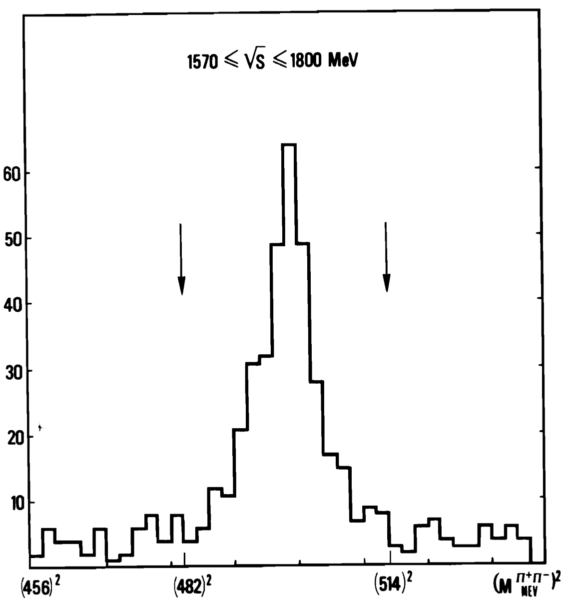

FIG.4 - Invariant mass of two particles assumed to be pions with a vertex at more than 6 mm from the beam line.

Luminosity measurement

The on-line measurement is done with small angle Bhabha scattering[2]. The final determination is achieved using large angle Bhabha scattering. The e^+e^- are contaminated by unidentified cosmic rays (3 % very accurately known), $\mu^+\mu^-$ (8 % estimated by QED) and $\pi^+\pi^-$ (giving a 1 % systematic error). The two determinations agree with each other within 10 %. To the statistical error on the luminosity measurement (100 Bhabha events/nb^{-1}) we add a 10 % systematic error for possible uncontrolled variations of detection efficiency.

Efficiency determination

For each channel the efficiency has been determined by a Monte-Carlo method taking into account the efficiency of detection of the MWPC and the production dynamics. As the detector does not cover a 4π solid angle, the efficiency may depend on the dynamics. We give the results for what we think are the likeliest dynamics and include as systematic errors the differences due to other possible dynamics. Radiative corrections of the Bremsstrahlung type were included in the Monte-Carlo calculation. These were calculated in the peaking approximation, using the formulas of Bonneau and Martin[3].

RESULTS

$p\bar{p}$ cross section (50 events)

Events selection for this channel could not be done for the whole solid angle since the cosmic-ray veto-system is not sufficiently efficient : cosmic-ray muons having the same momentum inside the apparatus as $p\bar{p}$ are stopped by the magnet coil or iron. We have used only the azimuthal range $-70° < \phi_p < 160°$, where cosmic-rays are scarce or enter the system through the scintillator in the direction of what we think to be the proton (a real proton cannot reach this scintillator at these energies). The signal obtained in the p_A distribution with the above cuts is quite clean (Fig. 5).

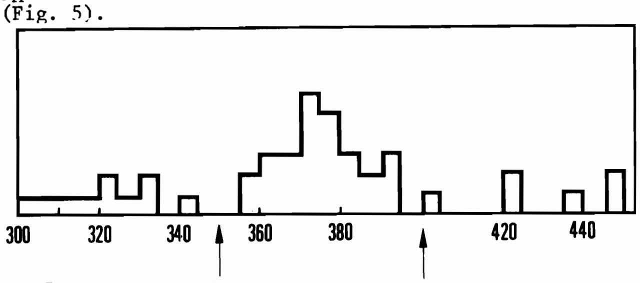

FIG.5 - Proton-Antiproton average momentum P_A for $2000 < \sqrt{S} < 2060$ MeV.

If one assumes identical electric and magnetic form factors, the overall detection efficiency is $\simeq$ 17%. The squared form factor versus energy, calculated under the same assumption, is shown in Fig. 6. Our time-like data and the previous measurements[4,5], are in fair agreement with estimates based on vector dominance models[11]. On the contrary, the well known dipole fit of the space-like data would give, in the time-like region, values (which are an order of magnitude lower than the measured ones) for the squared form factors.

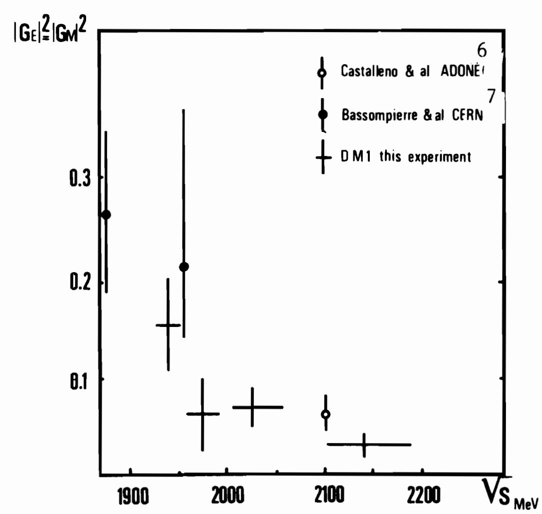

FIG.6 - $p\bar{p}$ form factor assuming $|G_E|^2 = |G_M|^2$

The question arises as to whether one of the previously reported[6] baryonium states at 1935 and 2020 MeV could be a 1^{--} resonant state decaying into e^+e^-. Our results give the following limits on $\Gamma_{e^+e^-} B_{p\bar{p}}$ for these two states within 95% confidence level.

m = 1935 MeV Γ = 9 MeV $\Gamma_{e^+e^-} B_{p\bar{p}} < 1\times10^{-5}$ MeV

m = 2020 MeV Γ = 24 MeV $\Gamma_{e^+e^-} B_{p\bar{p}} < 2.5\times10^{-5}$ MeV

K^+K^- and $K^o_SK^o_L$ cross section (200 and 20 events)

A clear K^+K^- signal is seen in the low energy region, $\sqrt{S} < 1700$ MeV (Fig. 7). In contrast to $p\bar{p}$,

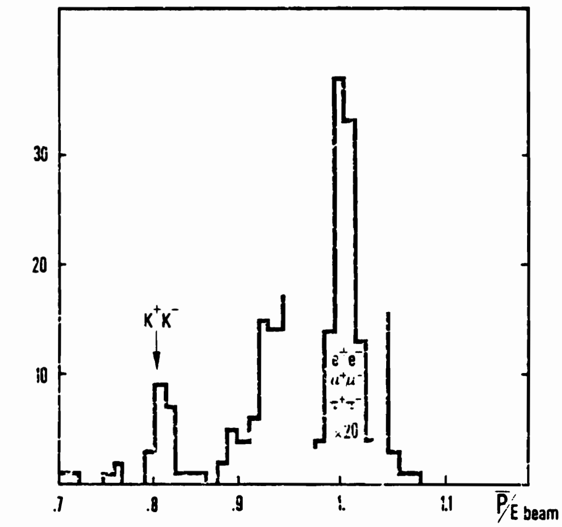

FIG.7 - Two charged body momentum spectrum for $1650 < \sqrt{S} < 1700$ MeV.

the K^+K^- detection efficiency (27%) can be determined without making any assumptions since there is only one form factor.

For the $K^o_SK^o_L$ channel a well-recognized K^o_S and a missing mass consistent with K^o_L are required (Fig. 8).

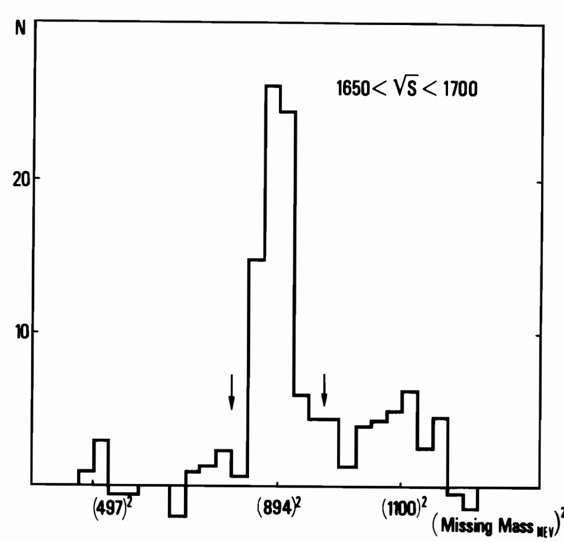

FIG.8 - K^S_o missing mass spectrum

The signal is very weak but without any background. The detection efficiency amounts to 14 %.

The K^+K^- and $K^o_S K^o_L$ form factors are shown in Fig. 9. In the low energy region, $\sqrt{S} < 1700$ MeV, the

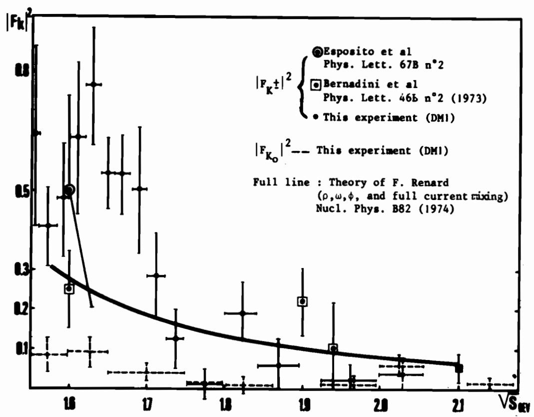

FIG.9 - Form factors of K^+K^- and $K^o_S K^o_L$.

$K^o_L K^o_S$ form factor is about 10 times less than the K^+K^- one. This implies a large interference effect between the isoscalar and isovector $\gamma \to K\bar{K}$ amplitudes, similar to what is expected from exact SU(3) symmetry for which the $K^o_S K^o_L$ form factor is zero. For $\sqrt{S} < 1700$ MeV the K^+K^- form factor is at least twice as large as the prediction obtained by F.M. Renard[7], which takes into account only the ρ^o, w, and ϕ contributions.
This form factor decreases quickly above 1700 MeV. In conclusion, the low mass ρ^o, ω, ϕ vector mesons are not sufficient to explain the K^+K^- and $K^o_S K^o_L$ form factor behaviour in this energy region.

$\pi^+\pi^-\pi^+\pi^-$ production (6000 events)

This channel has a rather large cross section in this energy range. Its dynamics are dominated by $\rho^o\pi^+\pi^-$ production (fig.10) but no clear structure is

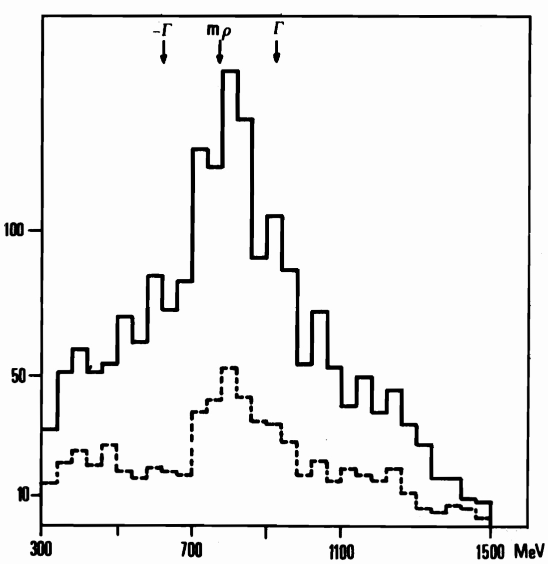

FIG.10 - Four charged pion events. Invariant mass of $\pi^+\pi^-$ pairs (4 entries/event) $2002 < \sqrt{S} < 2060$ MeV.
Full line : 3 and 4 visible track events.
Dashed line : 4 visible track events.

found in either the $\rho^o\pi^\pm$ invariant mass distribution or in the $\pi^+\pi^-$ mass recoiling against the ρ. The efficiency depends on the production dynamics, but is roughly the same for any simple dynamics as long as there is a ρ produced. At 1800 MeV we get 42.2% for pure phase space production and the following results under various assumptions about the ρ production dynamics: 48.5% for πA, (m=1100 MeV, Γ=300 MeV), 49.6% for ρ plus a $\pi^+\pi^-$ pair in s-wave, and 51.0% for ρE (m=1200 MeV, Γ=600 MeV). Thus, at each energy, we used the $\rho\pi\pi$ efficiency in computing the cross-section (Fig. 11). The results are not in disagreement with previous measurements[10,13], which were done without magnetic detection, and so involved the problem of removing the $K^+K^-\pi^+\pi^-$ contribution (see the discussion later in this paper).

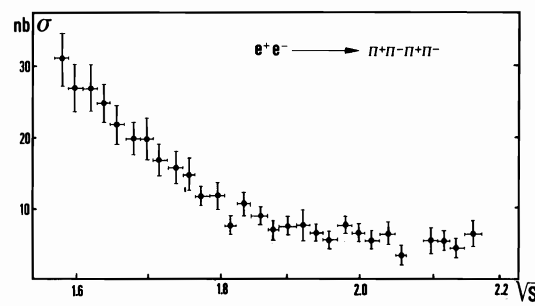

FIG.11 - Cross section of $\pi^+\pi^-\pi^+\pi^-$ production.

To obtain the quoted error we combined quadratically the statistical errors and an error of 10% for possible variations of detection efficiency. To these errors we must add a 12% systematic error for the dynamics and the luminosity determination.

The cross section is in agreement with the high energy part of the previously reported ρ'[9] and does not show any structure around 1700[10].

$\pi^+\pi^-\pi^+\pi^-\pi^o$ production (200 events)

In order to avoid contamination by $\pi^+\pi^-\pi^+\pi^-$, we selected events from a region of the missing momentum-missing mass scatter-plot where this contamination is sufficiently weak. We have not yet completely analysed the remaining contamination, and the cross section we give may be overestimated. However, in the 1570-1700 MeV energy range, about 70 % of the selected events come from $\omega^o\pi^+\pi^-$ production (Fig. 12). Thus, we are able to determine correctly the $\omega^o\pi^+\pi^-$ cross section. The efficiency depends only slightly on the production dynamics: 10.7% for $\omega\pi^+\pi^-$ in phase space and 9.9% for $\pi^+\pi^-\pi^+\pi^-\pi^o$ in phase space at 1650 MeV total energy.

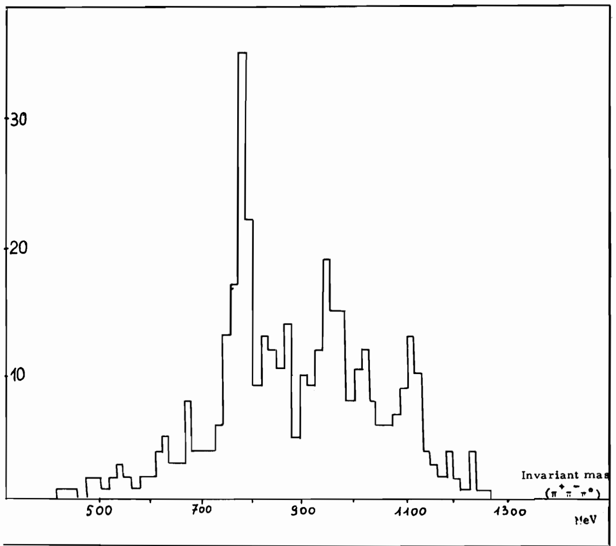

FIG.12 - $\pi^+\pi^-\pi^+\pi^-\pi^\circ$ events. Invariant mass of $\pi^+\pi^-\pi^\circ$ (4 entries/event).

The results given Fig.13 are not corrected for radiative effects. The average cross section in

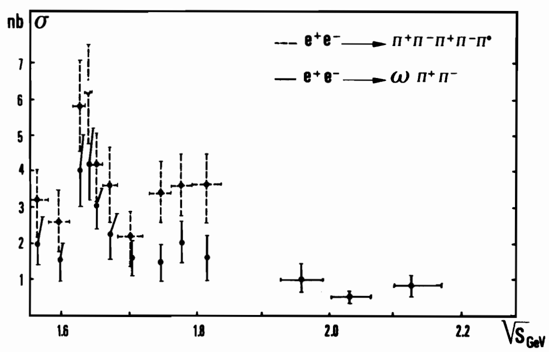

FIG.13 - Cross section of $\pi^+\pi^-\pi^+\pi^-\pi^\circ$ and $\omega^\circ\pi^+\pi^-$ productions. Radiative corrections are not yet applied.

the energy range 1550-1840 is at least a factor 2 lower than reported in reference 10. Nevertheless the $\omega^\circ\pi^+\pi^-$ data are compatible with the resonance structure previously seen near 1650 MeV[10], but we do not see any other structure.

$K^+K^-\pi^+\pi^-$ production (200 events)

The $K^+K^-\pi^+\pi^-$ events are well separated on the scatter-plot (Fig. 2) : they have zero total momentum and an apparent energy close to $\lambda\sqrt{S}$ (assigning four pion masses). λ varies with energy : .65 for $\sqrt{S} \simeq$ 1600 MeV to .8 for $\sim$ 2150 MeV. Although the particles are not individually identified, we are able to study the production dynamics : we choose from the 4 possibilities the mass assignment giving the best value for the reconstructed energy. Fig. 14 shows that the production is dominated by $K^{*\circ}K\pi$. No evident ρ structure appears in the high energy part (> 1925 MeV) of the data.

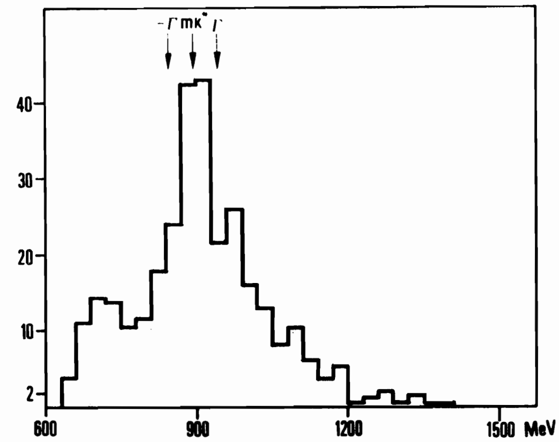

FIG.14 - $K^+K^-\pi^+\pi^-$ events - Invariant mass of $K^\pm\pi^\mp$ events (2 entries /event) 1775 MeV < $\sqrt{S}$ < 2174 MeV.

There is no evident structure in either the three-body mass spectra involving the $K^{*\circ}$ or the spectrum of the $K^\pm\pi^\pm$ mass recoiling against the K^{*o}. In particular the $K^{*o}\bar{K}^{*o}$ production, if any, is weak. Again the efficiency depends on dynamics (8.9% for pure phase space and 12.5% for K^{*o} with opposite $K\pi$ in s-wave at 2130 MeV), but is roughly the same for all simple dynamics producing K^{*o}. Thus we take this value for computing the cross section given in Fig. 15.

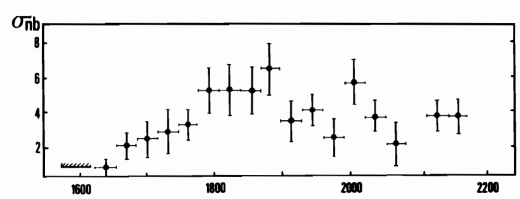

FIG.15 - Cross section of $K^+K^-\pi^+\pi^-$ productions.

Inclusive K^o_S production (550 events)

The efficiency for detecting a K^o_S decaying into $\pi^+\pi^-$ is slightly momentum dependent and is evaluated by a Monte-Carlo technique. The production angular distribution is assumed to be isotropic. In the low energy part ($\sqrt{S}$ < 1800 MeV), where the KK^* production is dominant, this assumption introduces at most 10 % systematic error. The detection efficiency is essentially zero below 120 MeV/c. This loss at low momentum is estimated from an extrapolation of the momentum spectrum to zero momentum. The correction amounts to 5 %. The data are corrected for the unobserved decay $K^o_S \to \pi^o\pi^o$.

In Fig. 16 the neutral kaon production is compared to muon pair production. The ratio $R_{K^o} = 2\sigma_{K^o_S}/\sigma_{\mu\mu}$ is given between 1570 and 2180 MeV, assuming an equal number of K_S and K_L.

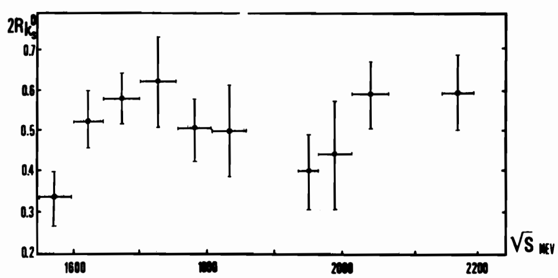

FIG.16 - R_{K_o}

In this energy region R_{K^o} stays almost constant. Its value, about .5, is somewhat higher than the .33 expected from the direct production of a $s\bar{s}$ pair by a photon, and lower than the 2/3 value given by the Feynman and Field jet model[12].

$K^o_S K^\pm\pi^\mp$ production (130 $K^o_S K^\pm\pi^\mp$ events and 200 $K^o_S K^{*o}$ events)

This channel is selected from events with 3 or 4 visible tracks- two of them compatible with a decay $K^o_S \to \pi^+\pi^-$. No cut on the flight distance of the K^o_S is necessary for the four prong events, as the contamination by other channels is small. We also require the reconstructed total energy assigning a $K^\pm$ mass and a $\pi^\mp$ mass to the two remaining tracks (one missing at most)- to be equal to the centre of mass energy within 2.5 %.

The measured $K^o_S K^\pm\pi^\mp$ cross-section is given in Fig. 17. It amounts to about 5 nb in the low energy region ($\sqrt{S}$ < 1700 MeV), and decreases quickly around 1800 MeV.

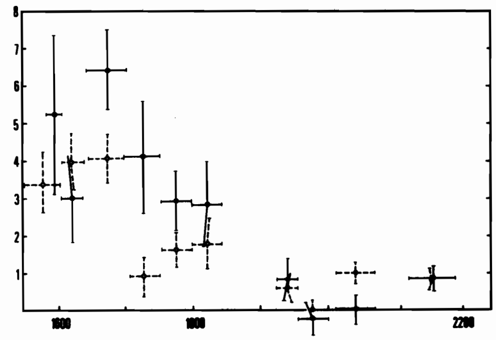

FIG.17 - Cross sections of $K^o_S K^\pm\pi^\mp$ and $K^o_S K^{*o}$ production.
Radiative corrections are not yet applied.
Full line : $K^o_S K^{*o}$
Dashed line : $K^o_S K^\pm\pi^\mp$

The Dalitz plot of the observed events shows a quasi two-body K^*K production mechanism for this channel (Fig. 18). The neutral $K^{*o}K^o$ production is much more important than the charged $K^{*\pm}K^\mp$ production. The ratio $K^{*o}K^o/K^{*\pm}K^\mp$ is compatible with what is expected in the exact SU(3) symmetry, i.e. $K^{*o}K^o/K^{*\pm}K^\mp = 4$.

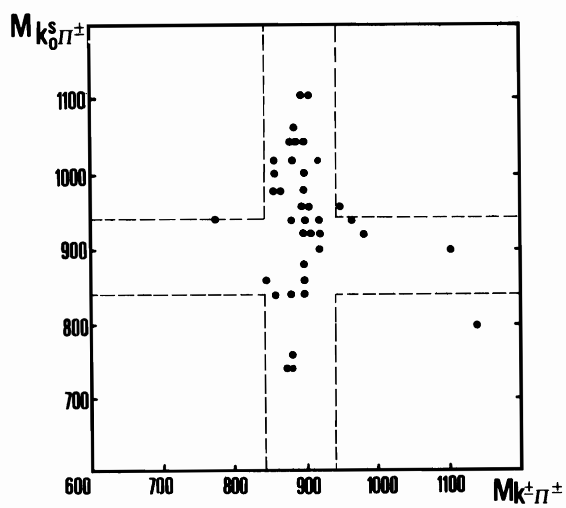

FIG.18 - Dalitz plot for $K^o_S K^\pm\pi^\mp$ events.

The $K_S^oK^{*o}$ channel is also selected by requiring only a clearly recognized K_S^o and a missing mass consistent with a K^{*o}. The $K_S^oK^{*o}$ cross-section is obtained by substracting the contamination from other channels, as seen on the missing mass spectrum (Fig. 8). The $K_S^oK^{*o}$ cross-section shows the same energy behaviour as the $K_S^oK^{\pm}\pi^{\mp}$ cross-section (Fig.17).

The ratio
$$r = \frac{\sigma\ (e^+e^- \to K_S^o\ K^{*o})}{\sigma\ (e^+e^- \to K_S^o\ K^{\pm}\ \pi^{\mp})}$$

is larger than one (Fig.19), i.e. compatible with the exact SU(3) prediction (r - 6/5), but larger than expected from a pure isospin (I = 0 or 1) production amplitude (r = 3/4). This shows again the large interference effect between the isoscalar and isovector amplitudes of the KK^* channel.

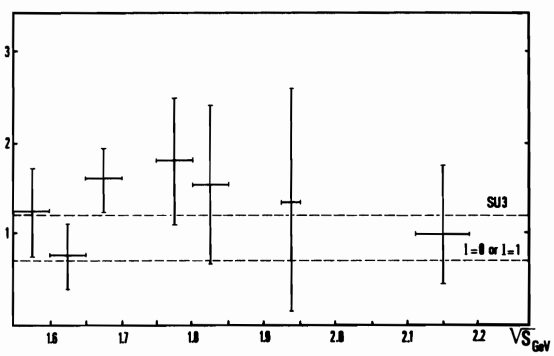

FIG. 19
The ratio $r = \sigma(e^+e^- \to K_S^oK^{*o})/\sigma(e^+e^- \to K_S^oK^{\pm}\pi^{\mp})$

Upper limits on ϕ production

We have examined K^+K^- pairs at the ϕ invariant mass in $K^+K^-\pi^+\pi^-$ events and get the upper limit, for $1775 < \sqrt{S} < 1840$ and $1925 < \sqrt{S} < 2200$,

$\sigma(\phi\pi^+\pi^-) < .5$ nb (90 % C.L.).

We have also looked for $\phi\pi^o$ and $\phi\eta^o$ in all two prong events with two non-aligned tracks : we assume that the two particles are K^+ and K^- and take the phase space for which the two kaons form a ϕ and the missing mass is consistent with a π^o or a η^o. We find, for $\sqrt{S} > 1700$ MeV,

$\sigma(\phi\pi^o) < 2$ nb (90 % C.L.)

$\sigma(\phi\eta^o) < 2$ nb (90 % C.L.).

REFERENCES

1. J. JEANJEAN et al., Nucl. Instr. and Meth. 117, 349 (1974).

A. CORDIER et al., Nucl. Instr. and Meth. 133, 237 (1976).

2. J.E. AUGUSTIN, Internal Report DCI 12-74

3. G. BONNEAU and F. MARTIN, Nucl. Phys. B27, 381 (1971)

4. M. CASTELLANO et al., Nuovo Cimento 14A, 1 (1973)

5. G. BASSOMPIERRE et al., Phys. Lett. 68B, 477 (1977).

6. A.S. CARROLL et al., Phys. Rev. Lett. 32, 247 (1974).

V. CHALOUPKA et al., Phys. Lett. 61B, 487 (1976).

W. BRÜCKNER et al., Phys. Lett. 67B, 222 (1977).

P. BENKHEIRI et al., Phys. Lett. 68B, 483 (1977).

7. F.M. RENARD, Nucl. Phys. B82, 1 (1974).

8. M. BERNARDINI et al., Phys. Lett. 46B 261 (1973)

9. See for example G.J. FELDMAN in Proceedings of the 19th International Conference on High Energy Physics (Tokyo 1978).

10. G. COSME et al., Nuclear Physics B 152, 215-231 (1979).

11. F.M. RENARD, Phys. Lett. 47B, 361 (1973).

S. BLATTNIK and N. ZOVKO, Acta Physica Austriaca 39, 62 (1974).

J.G. KÖRNER and M. KURODA, Phys. Rev. D16, 2165 (1977).

12. R.D. FIELD and R.P. FEYNMAN, Nuclear Physics B 136, 1 (1978).

13. B. ESPOSITO et al., Lett. Nuovo Cimento 19 (1977) 21.

B. ESPOSITO et al., Lett. Nuovo Cimento 25 (1979), 5.

DISCUSSION

Elliot Treadwell, Fermilab;

Have you compared $K^*\bar{K}^*$ mass spectrum with $K^*K\pi$ mass spectrum to observe the difference between an even G^- parity state and an odd G^- parity state ?

B.Delcourt: $K^*\bar{K}^*$ is very low.